

# Application of infrared photoacoustic spectroscopy in catalysis

J. Ryczkowski \*

*University of Maria Curie-Skłodowska, Faculty of Chemistry, Department of Chemical Technology, Pl. M. Curie-Skłodowskiej 3,  
20-031 Lublin, Poland*

Available online 6 March 2007

## Abstract

The analysis of solid samples can often be a difficult problem for the researchers dealing with infrared spectroscopy. In conventional absorption spectroscopy the measurement of absorption is transferred to a measurement of the radiation transmitted through the sample. On the contrary, in photoacoustic spectroscopy (PAS), the adsorbed radiation is determined directly via its heat and hence the sound produced in the sample. Fourier transform infrared PAS (FT-IR/PAS) is one of the main IR techniques which successfully can be applied in catalysis research. Examples of this spectroscopic technique application will be presented as well as some limits of its use.

© 2007 Elsevier B.V. All rights reserved.

**Keywords:** FT-IR/PAS; Catalysis

## 1. Introduction

Photoacoustics was pioneered by Bell in 1880. Following the reintroduction of photoacoustics as a spectroscopic tool by Rosencwaig and Gersho [1,2], the method was applied to a wide range of problems including those connected with surface science and catalysis. Bases of photoacoustics and PAS were extensively described in the book of Rosencwaig [3], which was edited in vol. 57 of Chemical Analysis Series (CAS). Next important books in this area were published by Bialkowski [4] (vol. 134 of CAS) and recently by Michaelian [5] (vol. 159 of CAS). IR/PAS is sometimes said to originate with the work of Busse and Bullemer [6], who obtained a PA spectrum of methanol vapor using a commercial FT-IR spectrometer and an absorption cell fitted with a microphone. However, first FT-IR/PAS spectrum of a solid was published by Rockley [7], who presented a single result for a polystyrene film in the mid-IR. More details about evolution of IR/PAS can be found in a book mentioned already [5].

## 2. Background

Photoacoustic (PA) measurements are unique in that they depend directly on the energy absorbed by the sample, rather

than on what is transmitted or reflected [8–10]. The sample is placed in a sealed chamber (Fig. 1).

When radiation is absorbed it is converted into heat which can be detected as a change of pressure in the gas (e.g. air, argon, helium) above the sample. This heat transfer process is sufficiently fast to follow the modulation of the radiation produced in an FT-IR spectrometer. Heat diffuses to the sample surface and into adjacent gas atmosphere. The thermal expansion of this gas produces the PA signal. The change in pressure is detected with a very sensitive microphone. A spectrum is obtained by ratioing the detector signal to that generated with a totally absorbing material such as carbon black. The spectrum comes from a surface layer and the effective penetration can be more than 100  $\mu\text{m}$ . This can result in total absorption for strong bands, so that relative intensities are distorted. It is interesting to remark that reflected or scattered light do not cause the PA signal. However, absorbed electromagnetic wave by the gases do it. The effective depth of penetration depends on the modulation frequency which varies with wavelength in rapid-scanning FT-IR spectrometers. In step-scan spectrometers the modulation frequency is constant for all wavelengths, so simplifying interpretation of the spectra. Some information about the depth distribution of different components can be obtained by varying the modulation frequency.

In practice, the main value of PA measurements has been in obtaining spectra from strongly absorbing samples such as carbon-like or opaque materials, and for materials that cannot

\* Tel.: +48 81 537 55 96; fax: +48 81 537 55 65.

E-mail address: [ryczkows@hermes.umcs.lublin.pl](mailto:ryczkows@hermes.umcs.lublin.pl).

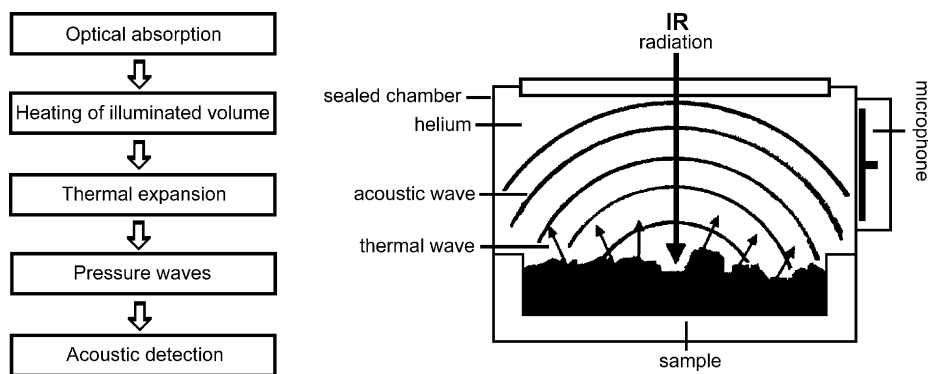


Fig. 1. Evaluation of PA signal and the principle of PA measurement.

be ground to a fine powder or be prepared with a flat surface. Sample preparation is minimal, requiring only that the specimen is small enough to fit in the chamber [8–10].

A significant number of books [3–5], book chapters [8–16], review articles [17–21], and texts in scientific journals [22–47] on FT-IR/PAS have been published during the last 25 years. Some of them contain general content of the use and application of FT-IR/PAS [22–31], others are more specific and are devoted to real-time PA parallel detection of products from catalyst libraries [32], step-scan and depth profiling analysis [33–40], the effect of particle size on FT-IR/PAS spectra [41–44], the temperature effect on PA signal [45], sample emission effects [46], and synchrotron IR/PAS [47]. During a PA measurement the sample is enclosed in a small, tightly closed sample compartment called PA cell [48–54]. Nowadays commercially available PA detector fits to most modern FT-IR spectrometers [55]. The summary of the FT-IR/PAS technique and its applications is extensively discussed by McClelland et al. [8–10] and Michaelian [5]. Chapter 6 of the book [5] is dedicated to various applications of IR/PAS, including carbons, coals, clays and clay minerals, and catalysis.

### 3. Spectroscopic investigations

A main advantage of PAS applied to solids is the fact that no elaborate sample preparation is required and unpolished sample surface pose no problems. Even spectra of strongly scattering samples can easily be measured. Hence PAS is technique to study weak bulk and surface absorption, to evaluate the level of absorbed energy in thin films, to measure the spectra of oxide films in metals, various powders, adsorbed organics, etc. PAS is expected to be rather sensitive to surface adsorption, especially if the substrate is transparent or highly reflective in the wavelength region in which the adsorbate absorbs.

As it was mentioned the history of FT-IR/PAS application for solids begun with the work of Rockley [7]. A successful application of this technique has been continuing for the investigations of powdered or porous samples [51–53], solids and surface species [54,56–61], chemisorbed species [62], catalysis [63]. Gardella et al. have demonstrated the capabilities of FT-IR/PAS to analyze catalytic systems, providing qualitative and quantitative analysis of both gas phase and adsorbed species. It has to be underline the applications of the

discussed technique for the investigation of industrial materials or studies having an influence on the industrial production [64]. Those studies covers an analysis of coatings [65,66], rapid determination of limestone in lime products [67], spectra of distillation fractions derived from syncrude heavy gas oil [68], light gas oil [69], post-extraction oil sand [70]. Yang and Simms [71] have compared PA, diffuse reflectance (DR) and transmission IR spectra of the studied carbon fibres. They have conclude that PA and DR methods differentiate the near-surface region of a carbon fibre from its bulk. Moreover both mentioned techniques are reliable qualitative analysis techniques for carbon fibres. Abdallah has applied FT-IR/PAS for two different purities of C<sub>60</sub> fullerenes [72]. Cimadevilla et al. have studied the influence of coal forced oxidation on technological properties of cokes produced at laboratory scale and weathered stockpiled coking coals [73,74]. Other studies were connected with modified carbons [75–78], carbon deposits [79,80], and carbonized silica surface [81].

Typical catalytic applications of FT-IR/PAS are connected with the studies of adsorption on the surface of various supports, characterization of the supports surface, metal supported catalysts or catalytic reactions [82–123]. Ando et al. have described structural studies of hydrogen and/or oxygen chemisorption on the surface of diamond powders [82]. PAS in the area of IR has been applied for the investigations of silica [83,84], nanoporous SiO<sub>x</sub> thin films [85,86], reactions of TCl<sub>4</sub> and Me<sub>3</sub>Al with silica surface [87], adsorption of organics on silica and alumina [88,89]. Following applications were connected with the adsorption of organophosphorus compounds on MgO [90], non-stoichiometry cerium oxide-based catalysts [91,92], acidity and the nature of acid sites of sulphated zirconia [93], PA reflection–absorption spectroscopy (PARAS) for IR analysis of thin films on metal surfaces [94], studies of adsorbed species on fine particle of metal and metal oxide [95], kinetic studies of the water–gas shift reaction in the presence of  $\alpha$ -Fe<sub>2</sub>O<sub>3</sub> [96], the interaction of gamma-iron oxide powder with organics [97], structural investigations of synthetic ferrihydrite nanoparticles doped with Si [98], nondestructive testing of copper corrosion layer formed in the atmosphere [99]. Mohamed and Vansant have studied structural and acidic properties of Cu/SiO<sub>2</sub> catalysts [100]. FT-IR/PAS has been applied for the characterization of solid polyelectrolyte membranes containing a textured platinum catalyst [101]. Oh and Nair have discussed spatially resolved,

quantitative, in situ, nondestructive measurements of the transport of organic molecules through a polycrystalline, anisotropic, nanoporous molecular sieve membrane [102]. Brown et al. have utilized several methods of sample preparation and FT-IR analysis techniques (including PAS) for the observation of a sorption interaction between a clay mineral and an organo-phosphonate [103]. FT-IR/PAS technique has been successfully applied for the studies of ethylenediaminetetraacetic acid (EDTA) and its derivatives interaction with the inorganic oxides surface [104–109]. Another unique application of this technique is for studies of MCM-41 template removal or its modification [110–112].

FT-IR/PAS has been employed for studying modification of chrysolite surface [113], characterization of natural zeolites–mordenite and clinoptilolite [114], structural and acidic characteristic of Cu–Ni modified acid-leached mordenites [115]. Highfield and Moffat have been applied FT-IR/PAS for characterization of a number of heteropoly compounds [116–119]. Riseman et al. [120] have studied pyridine adsorption on Mo/Al<sub>2</sub>O<sub>3</sub> and Co–Mo/Al<sub>2</sub>O<sub>3</sub> catalysts. El Shafei and Mokhtar

have observed the interaction between molybdena and silica [121]. Pyridine adsorbed on silica supported copper–molybdenum catalysts was the subject of Mohamed studies [122]. Zerlia et al. have studied zirconia supported rhodium carbonyl clusters [123].

The largest number of research papers which include FT-IR/PAS catalytic investigations belongs to two scientific groups chaired by Kemnitz [124–143] and Vansant [25,100,144–171]. Kemnitz et al. have applied FT-IR/PAS for pyridine adsorption [124] for the studies of surface acidity and the nature of acid sites in  $\gamma$ -alumina [125], sulfated zirconia [126–130], WO<sub>3</sub>/ZrO<sub>2</sub> catalysts [131], modified zirconium and titanium dioxides [132], highly dispersed vanadium-doped metal oxides [133], chromia materials [134–137], various MgF<sub>2</sub> catalysts [138–140], and aluminium fluorides [141–143]. In the case of Vansant and co-workers IR/PAS is mostly a supplementary technique in the studies conducted with: silica and/or silicas surface and silica gel [144–151], MoO<sub>x</sub> layer on the surface of silica [152], adsorption of VO(acac)<sub>2</sub> or V(acac)<sub>2</sub> on silica and alumina [153–155], controlled deposition of iron oxide on the

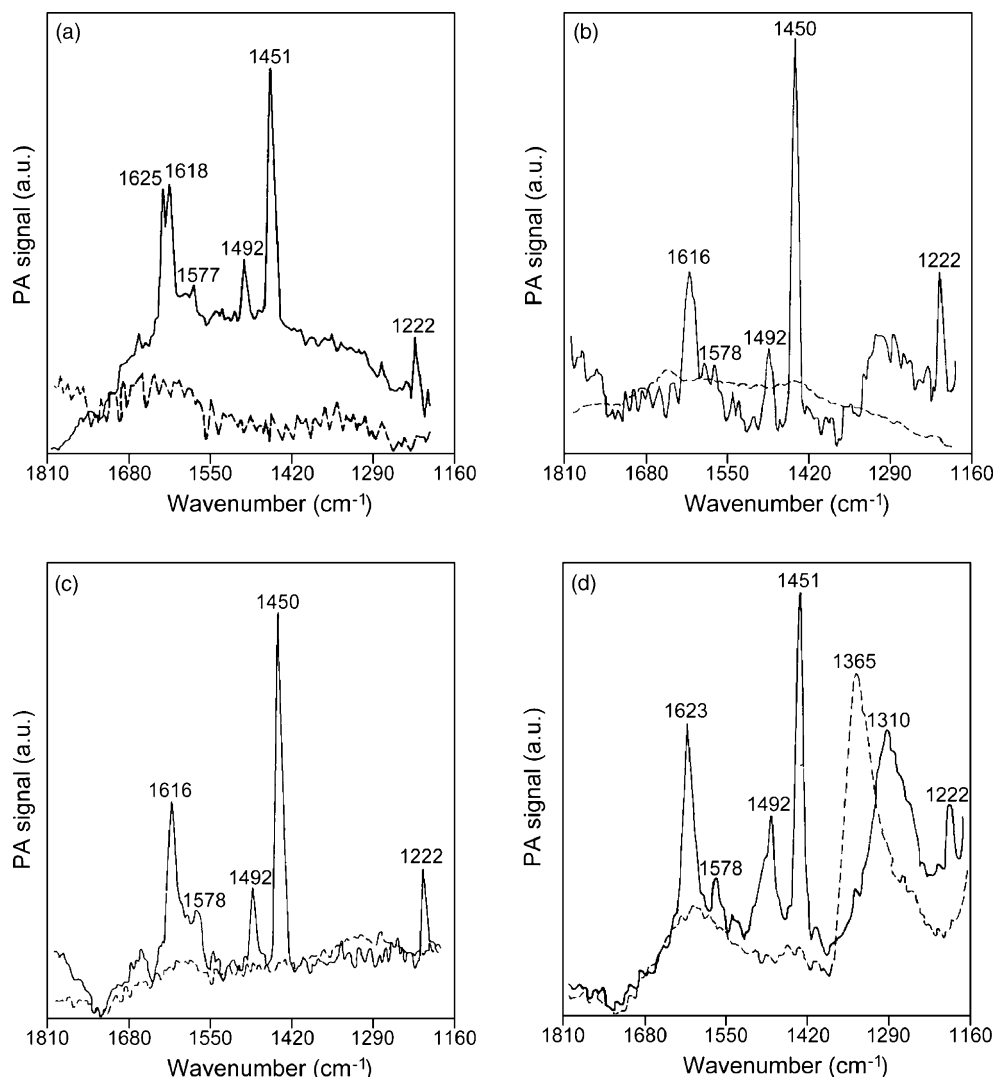


Fig. 2. FT-IR/PAS spectra of sulfided: (a) Al<sub>2</sub>O<sub>3</sub>, (b) Mo/Al<sub>2</sub>O<sub>3</sub>, (c) Co–Mo/Al<sub>2</sub>O<sub>3</sub>, and (d) Co/Al<sub>2</sub>O<sub>3</sub>, before and after exposure to pyridine (dashed and solid lines, respectively) [120].

surface of zirconia [156], vanadium oxide deposited on thermally stable mesoporous titania [157]. Following directions of Vansant group studies with FT-IR/PAS applications are related to the characterization of zeolites [158–160], porous clay and mesoporous silica materials [161–164] including MCM-48 [165,166], SB-15 and SBA-15 [167–171].

Some broader information about FT-IR/PAS applications are given below. Studies conducted by Riseman et al. [120] were undertaken to determine the presence of Brønsted and Lewis acid sites on the calcined and sulfided (Fig. 2) catalysts.

The IR/PA spectrum of pyridine adsorbed on the sulfided alumina support (Fig. 2a) itself shows two prominent bands (at 1625 and 1618  $\text{cm}^{-1}$ ) due to Lewis acidity. The FT-IR/PA spectrum of pyridine on sulfided  $\text{Mo}/\text{Al}_2\text{O}_3$  shown in Fig. 2b contain the Lewis band centered at 1616  $\text{cm}^{-1}$ . The narrower bands at 1450 and 1492  $\text{cm}^{-1}$  are invariant to the sulfiding treatment. The spectrum of pyridine on sulfided  $\text{Co-Mo}/\text{Al}_2\text{O}_3$  (Fig. 2c) is remarkably similar to that of sulfided  $\text{Mo}/\text{Al}_2\text{O}_3$  (Fig. 2b). When a sample containing  $\text{Co}/\text{Al}_2\text{O}_3$  was sulfided and exposed to pyridine, absorbances attributable to Lewis acidity were observed (Fig. 2d). The band of Lewis acidity occurs at 1623  $\text{cm}^{-1}$  and is much broader than those bands on sulfided  $\text{Co-Mo}/\text{Al}_2\text{O}_3$  (Fig. 2c), indicating complexation of pyridine on several types of anionic vacancies takes place. The band at 1492  $\text{cm}^{-1}$  is also significantly broader than those of the molybdena containing catalysts (Fig. 2b) also suggesting that chemisorption of pyridine occurs on cobalt centers as well as on  $\text{Al}^{3+}$  in various symmetries. The band centered around 1365  $\text{cm}^{-1}$  on the sample not exposed to pyridine is shifted to 1310  $\text{cm}^{-1}$  upon pyridine adsorption. This band apparently is insensitive to pretreatment conditions and the presence of Mo, supporting the conjecture that this absorbance arises from a surface cobalt phase associated with the alumina support only. For the sulfided catalysts, only Lewis acidity could be unambiguously identified. The lack of detectable Brønsted acidity on the sulfided catalyst under the experimental conditions employed does not necessarily rule out its presence under hydrosulfurization (HDS) reaction conditions. Some extended and more detailed information about FT-IR/PAS applications are given below.

Studies conducted by Riseman et al. [120] were undertaken to determine the presence of Brønsted and Lewis acid sites on the calcined and sulfided (Fig. 2) catalysts.

The IR/PA spectrum of pyridine adsorbed on the sulfided alumina support (Fig. 2a) itself shows two prominent bands (at 1625 and 1618  $\text{cm}^{-1}$ ) due to Lewis acidity. The FT-IR/PA spectrum of pyridine on sulfided  $\text{Mo}/\text{Al}_2\text{O}_3$  shown in Fig. 2b contain the Lewis band centered at 1616  $\text{cm}^{-1}$ . The narrower bands at 1450 and 1492  $\text{cm}^{-1}$  are invariant to the sulfiding treatment. The spectrum of pyridine on sulfided  $\text{Co-Mo}/\text{Al}_2\text{O}_3$  (Fig. 2c) is remarkably similar to that of sulfided  $\text{Mo}/\text{Al}_2\text{O}_3$  (Fig. 2b). When a sample containing  $\text{Co}/\text{Al}_2\text{O}_3$  was sulfided and exposed to pyridine, absorbances attributable to Lewis acidity were observed (Fig. 2d). The band of Lewis acidity occurs at 1623  $\text{cm}^{-1}$  and is much broader than those bands on sulfided  $\text{Co-Mo}/\text{Al}_2\text{O}_3$  (Fig. 2c), indicating complexation of pyridine on several types of anionic vacancies takes place. The

band at 1492  $\text{cm}^{-1}$  is also significantly broader than those of the molybdena containing catalysts (Fig. 2b) also suggesting that chemisorption of pyridine occurs on cobalt centers as well as on  $\text{Al}^{3+}$  in various symmetries. The band centered around 1365  $\text{cm}^{-1}$  on the sample not exposed to pyridine is shifted to 1310  $\text{cm}^{-1}$  upon pyridine adsorption. This band apparently is insensitive to pretreatment conditions and the presence of Mo, supporting the conjecture that this absorbance arises from a surface cobalt phase associated with the alumina support only. For the sulfided catalysts, only Lewis acidity could be unambiguously identified. The lack of detectable Brønsted acidity on the sulfided catalyst under the experimental conditions employed does not necessarily rule out its presence under hydrosulfurization (HDS) reaction conditions.

Mohamed has used pyridine adsorption to study the acid sites of silica supported  $\text{CuO-MoO}_3$  catalysts, with reference to  $\text{CuO}/\text{SiO}_2$  and  $\text{MoO}_3/\text{SiO}_2$  catalysts [122]. The spectra of pyridine adsorbed on the oxidized  $x$  wt.% of  $\text{CuO-9 wt.}\%$  of  $\text{Mo}/\text{SiO}_2$  catalysts (where  $x$  represents 1, 3, 6.6 and 15 wt.% of  $\text{CuO}$  loading, respectively) are shown in Fig. 3.

There are six major bands for 1 wt.% of  $\text{CuO-9 wt.}\%$  of  $\text{Mo}/\text{SiO}_2$  sample at 1450, 1487, 1574, 1608, 1538 and 1636  $\text{cm}^{-1}$ . These correspond to the bands of pyridine adsorbed on Lewis acid sites (1450, 1487, 1574 and 1608  $\text{cm}^{-1}$ ) and on Brønsted acid sites (1538 and 1636  $\text{cm}^{-1}$ ), respectively. As the copper oxide loading is increased, major changes in the bands occur. The disappearance of the band at 1537  $\text{cm}^{-1}$  is accomplished starting from 6.6 wt.% of  $\text{CuO}$ . Whereas the band at 1636  $\text{cm}^{-1}$

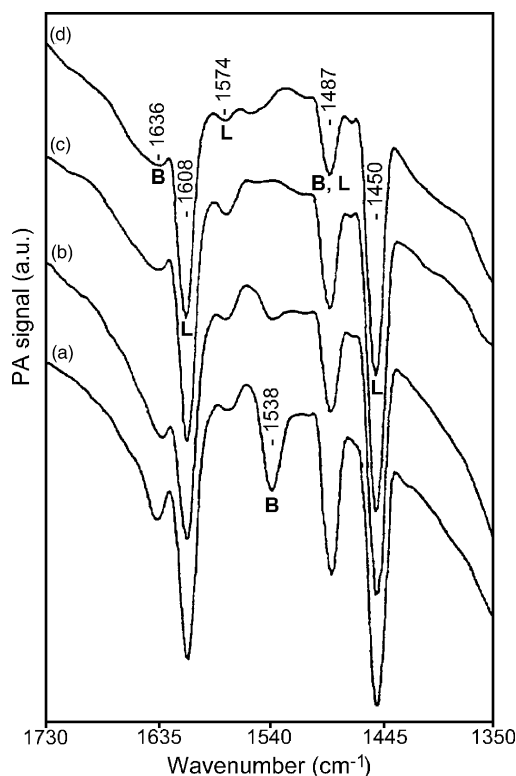


Fig. 3. FT-IR/PAS of pyridine adsorbed at 60 °C on oxidized catalysts supported on silica gel60: (a) 1 wt.%  $\text{CuO-9 wt.}\%$   $\text{MoO}_3$ , (b) 3 wt.%  $\text{CuO-9 wt.}\%$   $\text{MoO}_3$ , (c) 6.6 wt.%  $\text{CuO-9 wt.}\%$   $\text{MoO}_3$ , and (d) 15 wt.%  $\text{CuO-9 wt.}\%$   $\text{MoO}_3$  (L and B, Lewis and Brønsted acid centers, respectively) [122].

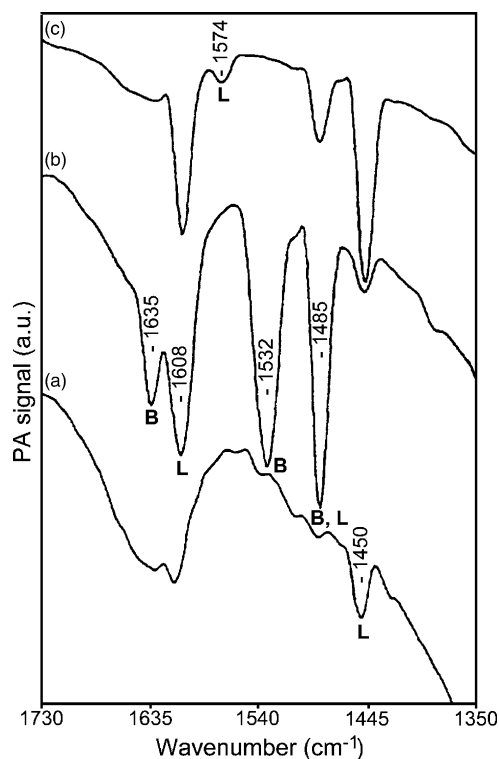


Fig. 4. FT-IR/PAS of pyridine adsorbed at 60 °C on the following catalysts supported on silica gel60: (a) 9 wt.% CuO/SiO<sub>2</sub> and (b) 9 wt.% MoO<sub>3</sub>/SiO<sub>2</sub>, 9 wt.% CuO–9 wt.% MoO<sub>3</sub>/SiO<sub>2</sub> (L and B, Lewis and Brønsted acid centers, respectively) [122].

is significantly decreased and shows a shift to a lower wave number, 1632 cm<sup>-1</sup>, upon increasing the wt.% of CuO. It is of interest to note also the significant increase of Lewis acidity over the Brønsted acidity for 1574 and 1608 cm<sup>-1</sup> bands upon increasing the copper oxide content. Furthermore, the strong band at 1487 cm<sup>-1</sup>, which represents both Lewis and Brønsted acidity, observed in both CuO/SiO<sub>2</sub> and MoO<sub>3</sub>/SiO<sub>2</sub> catalysts, shows a significant decrease as a result of increasing the copper loading. Fig. 4 shows the IR spectra of pyridine adsorbed on 9 wt.% of CuO/SiO<sub>2</sub>, 9 wt.% of MoO<sub>3</sub>/SiO<sub>2</sub> and 9 wt.% of CuO–9 wt.% of MoO<sub>3</sub>/SiO<sub>2</sub> catalysts.

Spectrum of 9 wt.% of CuO/SiO<sub>2</sub> catalyst (Fig. 4a), shows the band at 1450 cm<sup>-1</sup>, of a Lewis site, and the band at 1612 cm<sup>-1</sup> along with a small band at 1488 cm<sup>-1</sup>. Spectrum of 9 wt.% of MoO<sub>3</sub>/SiO<sub>2</sub> catalyst (Fig. 4b), generates both Lewis and Brønsted acid sites. The bands at 1635 and 1532 cm<sup>-1</sup> are assigned to pyridine adsorbed on Brønsted acid sites. The other bands in the spectrum (1608 and 1450 cm<sup>-1</sup>) are assigned to pyridine adsorbed on Lewis acid sites except the 1485 cm<sup>-1</sup> band which represents the contribution of both sites together. It is obvious that the intensity of the bands (either Lewis or Brønsted) in the 9 wt.% of MoO<sub>3</sub> sample exceeds that of the 9 wt.% of CuO sample. This reflects the enhancement of acid sites for Mo-silica compared with Cu-silica. It should be noted also that the 1450 cm<sup>-1</sup> band intensity (Fig. 4a and b) is more important on Cu-silica relative to Mo-silica and the strength of Lewis sites on Cu-silica is much higher than those on Mo-silica since the former is characterized by a band at 1612 cm<sup>-1</sup>

whereas the latter at 1608 cm<sup>-1</sup>. Spectrum of 9 wt.% of CuO–9 wt.% of MoO<sub>3</sub>/SiO<sub>2</sub> sample (Fig. 4c), shows bands at 1450, 1488, 1574 and 1608 cm<sup>-1</sup>. This spectrum reflects a new band at 1574 cm<sup>-1</sup> of Lewis acidity and the disappearance of 1635 and 1532 cm<sup>-1</sup> bands of Brønsted acid sites. The band at 1488 cm<sup>-1</sup> decreases in intensity and shifts to longer wavenumbers compared with the individual supported oxide catalyst. Furthermore, an extensive increase in intensity of the 1450 cm<sup>-1</sup> band is observed. As is evident from this spectrum (Fig. 4c), an increase in the number and strength of Lewis acid sites while a decrease of Brønsted acid sites is observed. The band of Lewis acidity observed at 1574 cm<sup>-1</sup> is attributed to the presence of CuMoO<sub>4</sub> species. This band is not observed in the individual oxide form of both CuO/SiO<sub>2</sub> and MoO<sub>3</sub>/SiO<sub>2</sub> catalysts.

Zerlia et al. [123] have studied CO hydrogenation catalyst precursors prepared by adsorbing Rh<sub>4</sub>(CO)<sub>12</sub> and Mo(CO)<sub>6</sub> on ZrO<sub>2</sub>. The FT-IR/PA spectrum of solid Rh<sub>4</sub>(CO)<sub>12</sub> (Fig. 5b) shows bands with maxima at 2066 and 2040 cm<sup>-1</sup> due to CO linearly bonded to Rh and a band at 1870 cm<sup>-1</sup> attributed to bridging CO.

A weak band of gaseous CO<sub>2</sub> at 2349 cm<sup>-1</sup> can also be noticed. Zirconia-supported Rh<sub>4</sub>(CO)<sub>12</sub> shows quite different IR features: in the region of linearly bonded CO three bands are observed at 2092, 2060 and 2015 cm<sup>-1</sup>, while the band of bridging CO is much weaker, compared with pure Rh<sub>4</sub>(CO)<sub>12</sub>,

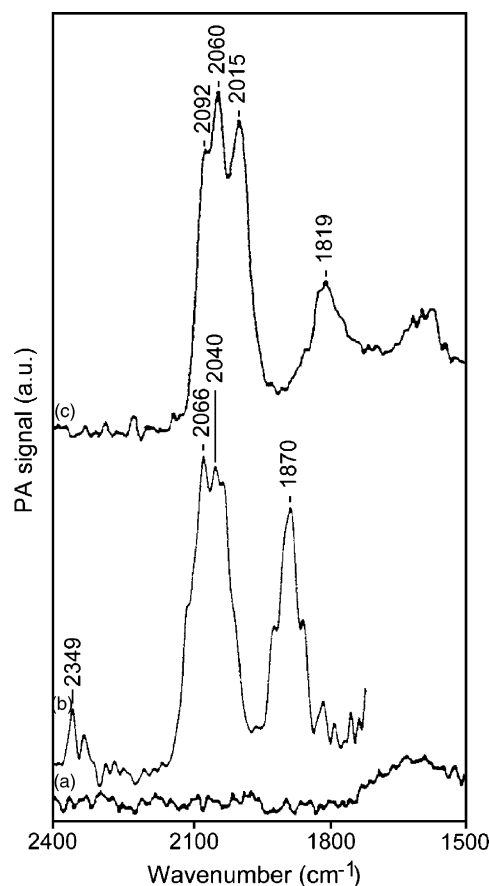


Fig. 5. FT-IR/PA spectra of: (a) ZrO<sub>2</sub>, (b) pure Rh<sub>4</sub>(CO)<sub>12</sub>, and (c) Rh<sub>4</sub>(CO)<sub>12</sub>/ZrO<sub>2</sub> [123].



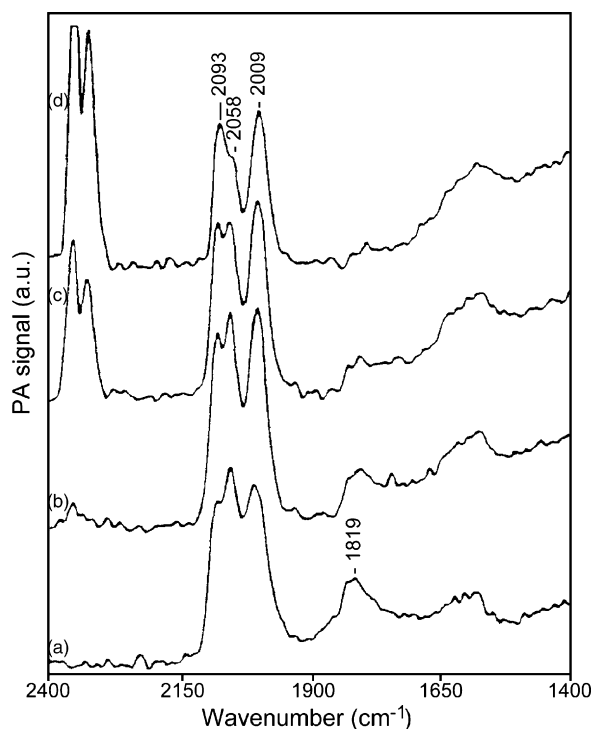


Fig. 6. FT-IR/PA spectra of  $\text{Rh}_4(\text{CO})_{12}/\text{ZrO}_2$  as a function of time at 32 °C: (a) after 1 min, (b) after 1 h, (c) after 4 h, and (d) after 22 h [123].

and shifted to 1819  $\text{cm}^{-1}$ . Moreover, the spectrum of the sample placed in the PA cell at about 32 °C under helium atmosphere exhibited a remarkable evolution (Fig. 6).

The band of bridging CO gradually decreased and disappeared after few hours; also the band of linearly bonded CO at 2060  $\text{cm}^{-1}$  decreased in intensity, while a band centered at 2349  $\text{cm}^{-1}$  due to  $\text{CO}_2$  gradually grew up. As a consequence, carbonates deposition occurred on the support, as suggested by a broad band at 1550–1650  $\text{cm}^{-1}$  (not shown). On the basis of the assignments reported for CO chemisorbed on  $\text{Rh}/\text{Al}_2\text{O}_3$ , the authors proposed a description of the complex surface structure of  $\text{Rh}_4(\text{CO})_{12}/\text{ZrO}_2$  [123].

In a study on the effect of additives on the catalytic activity of  $\text{Rh}/\text{ZrO}_2$  in CO hydrogenation, the authors observed that Mo exerts a strong promotion effect both on CO conversion and on selectivity to oxygenated products. To know more on this promotion effect of Mo, they have studied the catalyst precursor  $\text{Rh}_4(\text{CO})_{12} + \text{Mo}(\text{CO})_6/\text{ZrO}_2$  in the way similar to  $\text{Rh}_4(\text{CO})_{12}/\text{ZrO}_2$ . The IR spectrum of the sample containing an Rh/Mo ratio = 1:1 (Fig. 7) is relatively more complex, in the linear CO region, than that of the monometallic system (Fig. 6).

Gem-dicarbonyl, linear CO and bridging CO are visible as in  $\text{Rh}_4(\text{CO})_{12}/\text{ZrO}_2$ , but the band centered at 2026  $\text{cm}^{-1}$  shows two inflection points on the low frequency side. The spectra recorded after various time intervals show that the band initially centered at about 2026  $\text{cm}^{-1}$  gradually shrank and after 16 h the maximum was at 2013  $\text{cm}^{-1}$ . At that time, bridging CO almost disappeared, linear CO was still visible with a band at 2062  $\text{cm}^{-1}$ . The authors have concluded that FT-IR/PAS combined with TPD (temperature programming desorption) proved to be an efficient tool in describing the decomposition

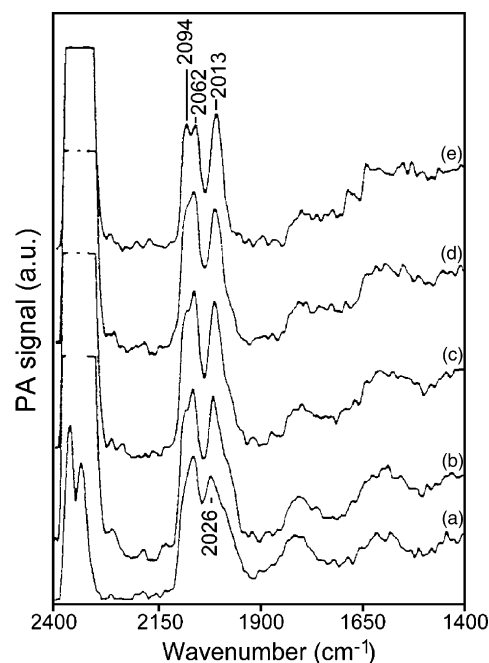


Fig. 7. FT-IR/PA spectra of  $\text{Rh}_4(\text{CO})_{12} + \text{Mo}(\text{CO})_6/\text{ZrO}_2$  (Rh/Mo = 1:1) as a function of time at 32 °C: (a) after 1 min, (b) after 1 h, (c) after 2 h, (d) after 3.5 h, and (e) after 16 h [123].

mechanism, which involves CO dissociation and oxidation of Rh by chemisorbed oxygen, with parallel evolution of  $\text{CO}_2$  [123].

Silica supported molybdenum oxide catalysts have been prepared by liquid and gas phase deposition, followed by calcination of the deposited molybdenyl acetylacetonato complex [152]. An evaluation of the molecular designed dispersion (MDD) method has been made by comparing the deposited molybdena structures obtained by the designed dispersion of  $\text{MoO}_2(\text{acac})_2$  with catalysts prepared by the conventional impregnation method using ammonium heptamolybdate. In the case of impregnated catalysts two samples were prepared with low and high Mo loading (Figs. 8 and 9, respectively).

The corresponding IR spectrum (Fig. 8B, spectrum b) shows absorption bands at 990  $\text{cm}^{-1}$ , 945  $\text{cm}^{-1}$  and shoulders at 954  $\text{cm}^{-1}$ , and 925  $\text{cm}^{-1}$ . The bands between 900 and 1000  $\text{cm}^{-1}$  are associated with terminal  $\nu(\text{Mo}=\text{O})$  vibrations of different oxide structures. The 990  $\text{cm}^{-1}$  frequency is characteristic for the terminal  $\nu(\text{Mo}=\text{O})$  vibration of crystalline orthorhombic  $\text{MoO}_3$ . The 945  $\text{cm}^{-1}$  band together with the 954  $\text{cm}^{-1}$  shoulder are ascribed to the terminal  $\nu(\text{Mo}=\text{O})$  vibrations of polymolybdates, indicating that different molybdenum oxide structures are present. The molybdena–silica interaction can be studied with IR spectroscopy by observing the (Si–O–Mo) absorption band at 925  $\text{cm}^{-1}$ . The tiny shoulder in Fig. 8B, spectrum b, suggests the presence of only a few (Mo–O–Si) bonds and therefore a rather poor interaction between the deposited Mo and the support. This observation is confirmed by a study of the hydroxyl region. Pure silica, preheated at 700 °C, exhibits only isolated silanols vibrating at 3745  $\text{cm}^{-1}$  (Fig. 8A, spectrum a). After the impregnation of the  $\text{MoO}_x$  species, the

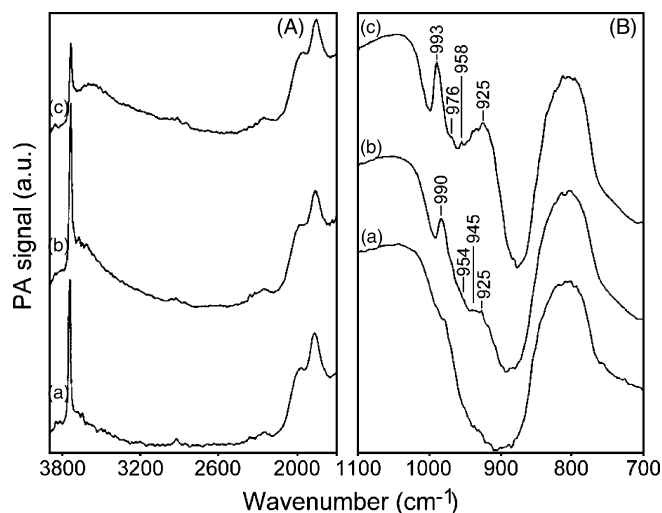


Fig. 8. Comparison of the IR absorption of: (a) silica pretreated at 700 °C, (b) a low loading impregnated catalyst, and (c) a low loading MDD catalyst. Shown are: A, the absorption in the range of the hydroxyl vibration and B, the low-frequency IR absorption [152].

intensity of these silanol vibrations has decreased very little, indicating that only a few (Si–O–Mo) bonds have been created.

The IR spectrum of the high loading catalyst (Fig. 9B, spectrum b) shows a very intense terminal  $\nu(\text{Mo}=\text{O})$  vibration at 993  $\text{cm}^{-1}$ , belonging to ortho-rhombic  $\text{MoO}_3$ .

The presence of polymolybdate species is supported by the presence of IR absorption bands at 976, 960 and 952  $\text{cm}^{-1}$ . The 976  $\text{cm}^{-1}$  frequency is an indication of the presence of silicomolybdic acid. The 960  $\text{cm}^{-1}$  band is associated with polymer structures of octahedral  $\text{MoO}_6$  units. The (Mo–O–Mo) bridges between those units exhibit an infrared band at 879  $\text{cm}^{-1}$ . The low intensity of this band excludes the formation of a large (Mo–O–Mo) network and suggests the presence of microcrystalline oxide structures on the substrate surface. In spite of these micro-crystallites, still more (Si–O–Mo) bonds are formed than

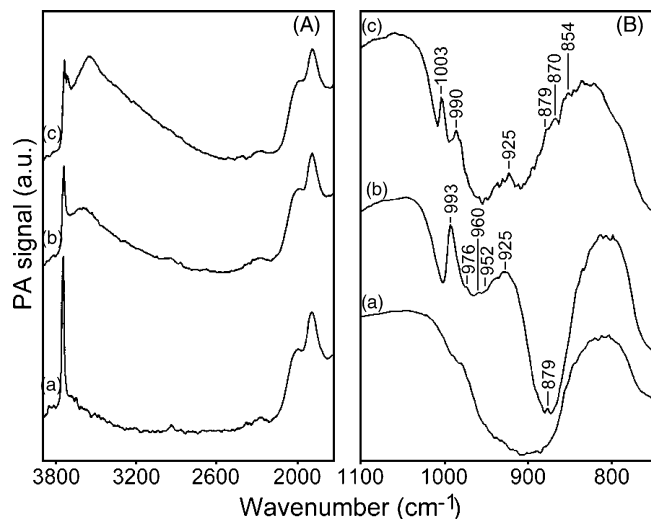


Fig. 9. Comparison of the IR absorption of: (a) silica pretreated at 700 °C, (b) a high loading impregnated catalyst, and (c) a high loading MDD catalyst. Shown are: A, the absorption in the range of the hydroxyl vibration and B, the low-frequency IR absorption [152].

on the low loading sample prepared by impregnation (Fig. 8B, spectrum b). This is deduced from the increased absorption of the (Mo–O–Si) vibration band, present as a shoulder at 925  $\text{cm}^{-1}$ . The better interaction between molybdena and silica can also be inferred from the loss of intensity of the isolated hydroxyl band at 3745  $\text{cm}^{-1}$  (Fig. 9A, spectrum b).

The authors have concluded that the MDD method results in a better grafting (more Si–O–Mo bonds) and thus a stronger metal oxide-support interaction than the conventional impregnation methods [152].

Baltes et al. [155] have studied alumina supported vanadium oxide catalysts prepared by the MDD method, using the vanadyl acetylacetonate complex— $\text{VO}(\text{acac})_2$ . The formation of the  $\text{VO}(\text{acac})_2$ -support material has been studied by both spectroscopic and chemical methods.

Fig. 10 shows the IR study of the  $\text{VO}(\text{acac})_2$  modified  $\gamma$ -alumina support. Fig. 10a presents the IR spectrum of the pure  $\gamma$ - $\text{Al}_2\text{O}_3$  after pretreatment at 400 °C. The basic hydroxy groups exhibit bands at 3780 and 3760  $\text{cm}^{-1}$ , the neutral hydroxy groups at 3730  $\text{cm}^{-1}$  and the acidic hydroxy groups exhibit bands at 3680 and 3560  $\text{cm}^{-1}$ . Fig. 10b–e present the IR spectra of the  $\text{VO}(\text{acac})_2$ - $\text{Al}_2\text{O}_3$  materials with increasing  $\text{VO}(\text{acac})_2$  loading. In Fig. 10b and c the intensity of the basic OH bands is reduced, due to an interaction with the vanadium complex. In the IR region 1600–1200  $\text{cm}^{-1}$  the characteristic acetylacetonate IR bands are present. The  $\text{VO}(\text{acac})_2$ - $\text{Al}_2\text{O}_3$  samples show a strong absorption at 1590  $\text{cm}^{-1}$ , whereas the pure  $\text{VO}(\text{acac})_2$  complex only shows a minor band at this position. This band is attributed to the  $\nu_s(\text{C}=\text{O})_{\text{ring}}$  vibration of

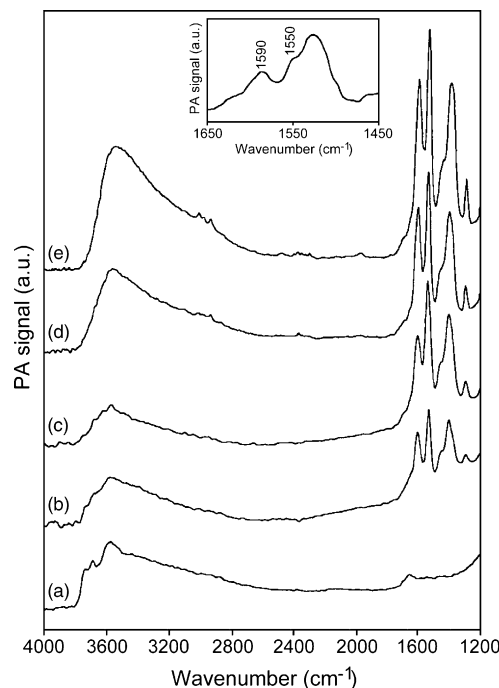


Fig. 10. FT-IR/PAS spectra of the  $\gamma$ - $\text{Al}_2\text{O}_3$  support pretreated at 400 °C: (a) before, and (b–e) after modification with  $\text{VO}(\text{acac})_2$ . Respective V loadings: (b) 0.1, (c) 0.2, (d) 0.3, and (e) 0.4 mmol/g. Inset: difference spectrum of modified alumina samples in parts (b) and (c), with respective vanadium loadings of 0.1 and 0.2 mmol/g [155].

an acac ligand. However, pure  $\text{VO}(\text{acac})_2$  shows only a minor band at this position, whereas pure  $\text{Al}(\text{acac})_3$  exhibits strong absorption at  $1590\text{ cm}^{-1}$ . Therefore, the band at  $1590\text{ cm}^{-1}$  reveals the presence of Al-acac species, which means that, during the reaction of  $\text{VO}(\text{acac})_2$  with the alumina surface, acac ligands are evolved. The decrease in intensity of the OH bands and the presence of Al-acac shows that a ligand exchange reaction occurs, which results in the formation of a covalently bonded vanadium species and the evolved acetylacetone (Hacac) subsequently reacts with the c.u.s. (coordinatively unsaturated)  $\text{Al}^{3+}$  sites to give Al-acac. However, with increasing  $\text{VO}(\text{acac})_2$  loading (Fig. 10d and e) the broadening of the band between  $3600$  and  $2800\text{ cm}^{-1}$  suggests the presence of a hydrogen bond interaction between the acac ligands of the complex and the surface hydroxy groups.

The inset in Fig. 10 shows the difference spectrum of the acetylacetone IR region of the alumina samples in Fig. 10b and c, with vanadium loading of  $0.1$  and  $0.2\text{ mmol/g}$ , respectively. The difference spectrum reveals that upon increasing the V loading from  $0.1$  to  $0.2\text{ mmol/g}$ , the band at  $1590\text{ cm}^{-1}$  increases, indicating an increased amount of Al-acac, originating from the ligand exchange reaction of  $\text{VO}(\text{acac})_2$ . The band at  $1550\text{ cm}^{-1}$  is assigned to the overtone out of plane vibration of the C–H stretching mode of an acetylacetone ligand coordinated to vanadium. This evidences that, besides the surface species with acac ligands coordinated to aluminium, there is also an increasing amount of surface species with the acac still coordinated to the vanadyl group.

Those study reveals that  $\text{VO}(\text{acac})_2$  complexes react preferentially with the hydroxyl groups of the alumina, and only to a limited extent with the c.u.s.  $\text{Al}^{3+}$  sites. In addition, the deposition of the  $\text{VO}(\text{acac})_2$  complex on the alumina surface yields different supported vanadium configurations as a function of the surface loading, due to both ligand exchange and hydrogen bond interactions.

#### 4. Summary

PAS measures a sample's absorbance spectrum directly with a controllable sampling depth and with little or no sample preparation. This rapid direct analysis capability is applicable to nearly all samples encompassing a wide range of absorbance strengths and physical forms. Among the other key features of PAS are that it is nondestructive, non-contact, applicable to macro- and microsamples, insensitive to surface morphology. It has a spectral range from the ultraviolet to far IR, and is operable in PA absorbance, diffuse reflectance, and transmission modes; and is capable of measuring spectra of all types of solids without exposure to air or moisture.

The main limits of this technique applied to surface chemistry and catalysis are the following [172]:

- it needs a gaseous atmosphere (air, Ar, He, etc.),
- the cell needs a microphone just near the sample so that the sample cannot be heated and activated conveniently,
- the  $s/n$  (signal to noise) ratio is rather low.

One of the advantages of this technique is relative low cost of the PA detector.

However, the disadvantage of the FT-IR/PAS is a limited possibility of in situ measurements, what is particularly of great importance in the catalytic investigations. Nevertheless, as a supplementary technique for catalytic investigations, FT-IR/PAS is a powerful tool for research in this area. Finally, it has to be stated that PA spectrometry is not exactly a surface spectroscopy, because the penetration of the thermal effect is always significant, although it depends on the scan speed. Thus, only when the surface-to-bulk ratio is very high, the  $s/n$  ratio is sufficiently good.

#### References

- [1] A. Rosencwaig, A. Gerso, *Science* 190 (1975) 556.
- [2] A. Rosencwaig, A. Gerso, *J. Appl. Phys.* 47 (1976) 64.
- [3] A. Rosencwaig, *Photoacoustics and Photoacoustic Spectroscopy*, John Wiley & Sons, Inc., New York, 1980.
- [4] S.E. Bialkowski, *Photothermal Spectroscopy Methods for Chemical Analysis*, John Wiley & Sons, Inc., New York, 1996.
- [5] K.H. Michaelian, *Photoacoustic Infrared Spectroscopy*, John Wiley & Sons, Inc., Hoboken, New Jersey, 2003.
- [6] G. Busse, B. Bullemer, *Infrared Phys.* 18 (1978) 631.
- [7] M.G. Rockley, *Chem. Phys. Lett.* 68 (1979) 455.
- [8] J.F. McClelland, R.W. Jones, S. Luo, L.M. Seaverson, in: P.B. Coleman (Ed.), *Practical Sampling Techniques for Infrared Analysis*, CRC Press, Inc., Boca Raton, 1993, pp. 107–144, Chapter 5.
- [9] J.F. McClelland, S.J. Bajic, R.W. Jones, L.M. Seaverson, in: F.M. Mirabella (Ed.), *Modern Techniques in Applied Molecular Spectroscopy*, John Wiley & Sons, Inc., New York, 1998, pp. 221–265, Chapter 6.
- [10] J.F. McClelland, R.W. Jones, S.J. Bajic, in: J.M. Chalmers, P.R. Griffiths (Eds.), *Handbook of Vibrational Spectroscopy*, vol. 2, John Wiley & Sons, Ltd., Chichester, 2002, pp. 1231–1251.
- [11] H. Gunzler, H.-U. Gremlich, *IR Spectroscopy. An Introduction*, Wiley-VCH, Weinheim, 2002, pp. 142–143.
- [12] W. Schmidt, *Optical Spectroscopy in Chemistry and Life Sciences. An Introduction*, Wiley-VCH, Weinheim, 2005, Chapter. 7, pp. 253–273.
- [13] D.W. Vidrine, in: J.R. Ferraro, L.J. Basile (Eds.), *Fourier Transform Infrared Spectroscopy: Applications to Chemical Systems*, vol. 3, Academic Press, New York, 1982, pp. 125–148, Chapter 4.
- [14] J.R. Ferraro, in: D.R. Rossington, R.A. Condrate, R.L. Snyder (Eds.), *Advances in Materials Characterization*, Plenum Publishing Corp, 1983, pp. 171–198.
- [15] E.M. Eyring, S.M. Risemann, F.E. Massoth, in: T.E. Whyte, et al. (Eds.), *Catalytic Materials: Relationship Between Structure and Reactivity*, American Chemical Society, ACS Symposium Series No. 248, 1984, pp. 399–410, Chapter. 20.
- [16] J.B. Benziger, S.J. McGovern, B.S.H. Royce, in: M.L. Deviney, J.L. Gland (Eds.), *Catalyst Characterization Science*, American Chemical Society, ACS Symposium Series No. 288, 1985, pp. 449–463, Chapter. 38.
- [17] E.P.C. Lai, B.L. Chan, M. Hadjmohammadi, *Appl. Spectrosc. Rev.* 21 (1985) 179.
- [18] J. Ryzkowski, *Catal. Today* 68 (2001) 263, General.
- [19] J. Ryzkowski, S. Pasieczna, *Annales UMCS, Sectio AA Chemia*, LVII (2002) 281, Review.
- [20] S. Pasieczna, J. Ryzkowski, *J. Phys. IV* 109 (2003) 65, Review.
- [21] J. Ryzkowski, S. Pasieczna, *J. Phys. IV* 109 (2003) 79., Review.
- [22] D.G. Mead, S.R. Lowry, C.R. Anderson, *Int. J. Infrared Millimeter Waves* 2 (1981) 23.
- [23] H. Coufal, J.F. McClelland, *J. Mol. Struct.* 173 (1988) 129.
- [24] J. Mink, *Acta Phys. Hung.* 61 (1987) 71.
- [25] T. Linsen, K. Cassiers, P. Cool, E.F. Vansant, *Adv. Colloid Interface Sci.* 103 (2003) 121.



- [26] L. Rintoul, H. Panayiotou, S. Kokot, G. George, G. Cash, R. Frost, T. Bui, P. Fredericks, *Analyst* 123 (1998) 571.
- [27] R.D. Snook, *Analyst* 125 (2000) 45.
- [28] T. Schmid, *Anal. Bioanal. Chem.* 384 (2006) 1071.
- [29] J.F. McClelland, *Anal. Chem.* 55 (1983) 89A.
- [30] D. Noble, *Anal. Chem.* 66 (1994) 757A.
- [31] C. Haisch, R. Niessner, *Spectrosc. Eur.* 15 (2002) 10.
- [32] T. Johann, A. Brenner, M. Schwickardi, O. Busch, F. Marlow, S. Schunk, F. Schuth, *Angew. Chem. Int. Ed.* 41 (2002) 2966.
- [33] D.L. Drapcho, R. Curbelo, E.Y. Jiang, R.A. Crocombe, W.J. McCarthy, *Appl. Spectrosc.* 51 (1997) 453.
- [34] M.W.C. Wahls, J.P. Toutenhoofd, L.H. Leyte-Zuiderweg, J. de Bleijser, J.C. Leyte, *Appl. Spectrosc.* 51 (1997) 552.
- [35] E.Y. Jiang, W.J. McCarthy, D.L. Drapcho, R.A. Crocombe, *Appl. Spectrosc.* 51 (1997) 1736.
- [36] M.W.C. Wahls, J.C. Leyte, *Appl. Spectrosc.* 52 (1998) 123.
- [37] V.G. Gregoriou, S.E. Rodman, *Anal. Chem.* 74 (2002) 2361.
- [38] R.W. Jones, J.F. McClelland, *Appl. Spectrosc.* 50 (1996) 1258.
- [39] E.Y. Jiang, W.J. McCarthy, D.L. Drapcho, *Spectrosc.* 13 (1998) 21.
- [40] I. Noda, *Vibr. Spectrosc.* 36 (2004) 143.
- [41] P.S. Belton, R.H. Wilson, A.M. Saffa, *Anal. Chem.* 59 (1987) 2378.
- [42] R.S. Pandurangi, M.S. Seehra, *Anal. Chem.* 62 (1990) 1943.
- [43] N.L. Rockley, M.K. Woodard, M.G. Rockley, *Appl. Spectrosc.* 38 (1984) 329.
- [44] L. Fangxin, Y. Jinlong, *Phys. Rev. B* 55 (1997) 8847.
- [45] M.W. Urban, J.L. Koenig, *Anal. Chem.* 60 (1988) 2408.
- [46] S. McGovern, B.S.H. Royce, J. Benziger, *Appl. Opt.* 24 (1985) 1512.
- [47] K.H. Michaelian, R.S. Jackson, Ch.C. Homes, *Rev. Sci. Instrum.* 72 (2001) 4331.
- [48] J.B. Kinney, R.H. Staley, *Anal. Chem.* 55 (1983) 343.
- [49] N. Teramae, S. Tanaka, *Anal. Chem.* 57 (1985) 95.
- [50] T. Bruno, *Appl. Spectrosc. Rev.* 34 (1999) 91.
- [51] S.J. McGovern, B.S.H. Royce, J.B. Benziger, *Appl. Surf. Sci.* 18 (1984) 401.
- [52] S.J. McGovern, B.S.H. Royce, J.B. Benziger, *J. Appl. Phys.* 57 (1985) 1710.
- [53] J.-P. Monchalain, L. Bertrand, G. Rousset, F. Lepoutre, *J. Appl. Phys.* 56 (1984) 190.
- [54] K. Krishnan, *Appl. Spectrosc.* 35 (1981) 549, FT-IR/PAS of solids and cell.
- [55] <http://www.mtecpas.com>.
- [56] M.J.D. Low, G.A. Parodi, *Appl. Spectrosc.* 34 (1980) 76.
- [57] D.W. Vidrine, *Appl. Spectrosc.* 34 (1980) 314.
- [58] M.G. Rockley, *Appl. Spectrosc.* 34 (1980) 405.
- [59] S.O. Kanstad, P.-E. Nordal, *Infrared Phys.* 19 (1979) 413.
- [60] P.-E. Nordal, S.O. Kanstad, *Int. J. Quantum Chem.* 12 (Suppl. 2) (1977) 115.
- [61] J.F. McClelland, S. Luo, R.W. Jones, L.M. Seaverson, *SPIE* 1575 (1991) 226.
- [62] C. Morterra, M.J.D. Low, A.G. Severdia, *Appl. Surf. Sci.* 20 (1985) 317.
- [63] J.A. Gardella Jr., D.-Z. Jiang, W.P. McKenna, E.M. Eyring, *Appl. Surf. Sci.* 15 (1983) 36.
- [64] K.H. Michaelian, *Rev. Sci. Instrum.* 74 (2003) 659.
- [65] A.J. Vreugdenhil, M.S. Donley, N.T. Grebasch, R.J. Passinault, *Prog. Org. Coat.* 41 (2001) 254.
- [66] E. Almeida, M. Balmayore, T. Santos, *Prog. Org. Coat.* 44 (2002) 233.
- [67] G.A. Norton, J.F. McClelland, *Miner. Eng.* 10 (1997) 237.
- [68] K.H. Michaelian, R.H. Hall, J.T. Bulmer, *Spectrochim. Acta A* 59 (2003) 811.
- [69] K.H. Michaelian, R.H. Hall, J.T. Bulmer, *Spectrochim. Acta A* 59 (2003) 2971.
- [70] K.H. Michaelian, R.H. Hall, K.I. Kenny, *Spectrochim. Acta A* 64 (2006) 703.
- [71] Ch.Q. Yang, J.R. Simms, *Fuel* 74 (1995) 543.
- [72] S. Abdallah, *Egypt J. Solids* 27 (2004) 251.
- [73] J.L.G. Cimadevilla, R. Alvarez, J.J. Pis, *Fuel Process. Technol.* 87 (2005) 1.
- [74] J.L.G. Cimadevilla, R. Alvarez, J.J. Pis, *Vibr. Spectrosc.* 31 (2003) 133.
- [75] S. Pasieczna, J. Ryzkowski, J.L. Figueiredo, *Ann. Pol. Chem. Soc.* 2 (2003) 1251.
- [76] J. Ryzkowski, S. Pasieczna, J.L. Figueiredo, M.F.R. Pereira, T. Borowiecki, *J. Phys. IV* 117 (2004) 57.
- [77] M. Hofman, S. Pasieczna, L. Wachowski, J. Ryzkowski, *J. Phys. IV* 129 (2005) 225.
- [78] M. Hofman, L. Wachowski, S. Pasieczna, J. Ryzkowski, *J. Phys. IV* 137 (2006) 287.
- [79] S. Pasieczna, J. Ryzkowski, T. Borowiecki, K. Stolecki, *J. Phys. IV* 117 (2004) 41.
- [80] J. Ryzkowski, S. Pasieczna, K. Stolecki, T. Borowiecki, *J. Phys. IV* 137 (2006) 325.
- [81] V.A. Pokrovskiy, R. Leboda, V.V. Turov, B. Charnas, J. Ryzkowski, *Carbon* 37 (1999) 1039.
- [82] T. Ando, S. Inoue, M. Ishii, M. Kamo, Y. Sato, O. Yamada, T. Nakano, *J. Chem. Soc., Faraday Trans.* 89 (1993) 749.
- [83] D.J. Schwerha, Ch.-S. Orr, B.T. Chen, S.C. Soderholm, *Anal. Chim. Acta* 457 (2002) 257.
- [84] A.M. Saffa, K.H. Michaelian, *Appl. Spectrosc.* 48 (1994) 871.
- [85] D.-Q. Yang, M. Meunier, E. Sacher, *Appl. Surf. Sci.* 252 (2005) 1197.
- [86] D.-Q. Yang, M. Meunier, E. Sacher, *J. Appl. Phys.* 98 (2005) 114310.
- [87] J.B. Kinney, R.H. Staley, *J. Phys. Chem.* 87 (1983) 3735.
- [88] S.M. Riseman, F.E. Massoth, G.M. Dhar, E.M. Eyring, *J. Phys. Chem.* 86 (1982) 1760.
- [89] D.A. Saucy, G.E. Cabaniss, R.W. Linton, *Anal. Chem.* 57 (1985) 876.
- [90] Y.-X. Li, J.R. Schlup, K.J. Klabunde, *Langmuir* 7 (1991) 1394.
- [91] J.Y. Ying, A. Tschope, *Chem. Eng. J.* 64 (1996) 225.
- [92] J.Y. Ying, A. Tschope, D. Levin, *Nanostruct. Mater.* 6 (1995) 237.
- [93] H.K. Mishra, K.M. Parida, *Appl. Catal. A: Gen.* 224 (2002) 179.
- [94] S.O. Kanstad, P.-E. Nordal, *Appl. Surf. Sci.* 5 (1980) 286.
- [95] Y. Nakao, H. Yamada, M. Yamada, *SPIE* 1575 (1991) 538.
- [96] S.-J. Kim, I.-S. Byun, H.-Y. Han, H.-L. Ju, S.H. Lee, J.-G. Choi, *Appl. Catal. A: Gen.* 234 (2002) 35.
- [97] Y. Nishikawa, K. Kimura, A. Matsuda, T. Kenpo, *Appl. Spectrosc.* 46 (1992) 1695.
- [98] M.S. Seehra, P. Roy, A. Raman, A. Manivannan, *Solid State Commun.* 130 (2004) 597.
- [99] A.O. Salnick, W. Faubel, *Appl. Spectrosc.* 49 (1995) 1516.
- [100] M.M. Mohamed, E.F. Vansant, *Colloids Surf. A: Physicochem. Eng. Aspects* 96 (1995) 253.
- [101] D.G. Bessarabov, W. Michaels, R.D. Sanderson, *J. Membr. Sci.* 194 (2001) 135.
- [102] W. Oh, S. Nair, *Appl. Phys. Lett.* 87 (2005) 151912.
- [103] J.M. Brown, S.V. Compton, M.S. Blanche, *Anal. Chem.* 61 (1989) 2047.
- [104] J. Ryzkowski, *Proc. SPIE* 2089 (1993) 182.
- [105] J. Ryzkowski, T. Borowiecki, D. Nazimek, *Adsorp. Sci. Technol.* 14 (1996) 113.
- [106] J. Ryzkowski, *Vibr. Spectrosc.* 34 (2004) 247.
- [107] J. Ryzkowski, *Appl. Surf. Sci.* 252 (2005) 813.
- [108] J. Ryzkowski, *Vibr. Spectrosc.* 43 (2007) 203.
- [109] S. Pasieczna, J. Ryzkowski, *J. Phys. IV* 137 (2006) 321.
- [110] J. Ryzkowski, J. Goworek, T. Borowiecki, W. Gac, S. Pasieczna, *Thermochim. Acta* 434 (2005) 2.
- [111] W.M. Buda, S. Pasieczna, J. Ryzkowski, J. Goworek, *J. Phys. IV* 129 (2005) 207.
- [112] A. Kierys, S. Pasieczna, J. Ryzkowski, J. Goworek, *J. Phys. IV* 137 (2006) 291.
- [113] E. Mendelovici, R.L. Frost, J.T. Klopogrog, *J. Colloid Interface Sci.* 238 (2001) 273.
- [114] O. Korkuna, R. Leboda, J. Skubiszewska-Zięba, T. Vrublev'ska, V.M. Gun'ko, J. Ryzkowski, *Microporous Mesoporous Mater.* 87 (2006) 243.
- [115] M.M. Mohamed, *J. Colloid Interface Sci.* 265 (2003) 106.
- [116] J.G. Highfield, J.B. Moffat, *J. Catal.* 88 (1984) 177.
- [117] J.G. Highfield, J.B. Moffat, *J. Catal.* 89 (1984) 185.
- [118] J.G. Highfield, J.B. Moffat, *J. Catal.* 95 (1985) 108.
- [119] J.B. Moffat, J.G. Highfield, *Stud. Surf. Sci. Catal.* 19 (1984) 77.
- [120] S.M. Riseman, S. Bandyopadhyay, F.E. Massoth, E.M. Eyring, *Appl. Catal.* 16 (1985) 29.
- [121] G.M.S. El Shafei, M. Mokhtar, *Colloids Surf. A: Physicochem. Eng. Aspects* 94 (1995) 267.

- [122] M.M. Mohamed, *Spectrochim. Acta* 51A (1995) 1.
- [123] T. Zerlia, A. Carimati, S. Marengo, S. Martinengo, L. Zanderighi, *Stud. Surf. Sci. Catal.* 48 (1989) 943.
- [124] E. Kemnitz, A. Hess, G. Rother, S. Troyanov, *J. Catal.* 159 (1996) 332.
- [125] E. Kemnitz, A. Kohne, E. Lieske, *J. Fluorine Chem.* 81 (1997) 197.
- [126] J. Deutsch, V. Quaschnig, E. Kemnitz, A. Auroux, H. Ehwald, H. Lieske, *Topics Catal.* 13 (2000) 281.
- [127] V. Quaschnig, A. Auroux, J. Deutsch, H. Lieske, E. Kemnitz, *J. Catal.* 203 (2001) 426.
- [128] K. Parida, V. Quaschnig, E. Lieske, E. Kemnitz, *J. Mater. Chem.* 11 (2001) 1903.
- [129] H.A. Prescott, M. Wloka, E. Kemnitz, *J. Mol. Catal. A: Chem.* 223 (2004) 67.
- [130] J. Deutsch, H.A. Prescott, D. Muller, E. Kemnitz, H. Lieske, *J. Catal.* 231 (2005) 269.
- [131] R. Sakthivel, H. Prescott, E. Kemnitz, *J. Mol. Catal. A: Chem.* 223 (2004) 137.
- [132] A. Hess, E. Kemnitz, *Appl. Catal. A: Gen.* 149 (1997) 373.
- [133] K. Scheurell, E. Hoppe, K.-W. Brzezinka, E. Kemnitz, *J. Mater. Chem.* 14 (2004) 2560.
- [134] T. Skapin, E. Kemnitz, *J. Non-Cryst. Solids* 225 (1998) 163.
- [135] B. Adamczyk, O. Boese, N. Weiher, S.L.M. Schroeder, E. Kemnitz, *J. Fluorine Chem.* 101 (2000) 239.
- [136] T. Skapin, *J. Non-Cryst. Solids* 285 (2001) 128.
- [137] Y. Zhu, K. Fiedler, St. Rudiger, E. Kemnitz, *J. Catal.* 219 (2003) 8.
- [138] J.K. Murthy, U. Groß, S. Rudiger, E. Unveren, E. Kemnitz, *J. Fluorine Chem.* 125 (2004) 937.
- [139] J.K. Murthy, U. Gross, S. Rudiger, E. Kemnitz, *Appl. Catal. A: Gen.* 278 (2004) 133.
- [140] J.K. Murthy, U. Gross, S. Rudiger, E. Unveren, W. Unger, E. Kemnitz, *Appl. Catal. A: Gen.* 282 (2005) 85.
- [141] A. Hess, E. Kemnitz, *J. Catal.* 149 (1994) 449.
- [142] K. Scheurell, E. Kemnitz, *J. Mater. Chem.* 15 (2005) 4845.
- [143] S. Rudiger, U. Groß, M. Feist, H.A. Prescott, S.Ch. Shekar, S.I. Troyanov, E. Kemnitz, *J. Mater. Chem.* 15 (2005) 588.
- [144] N.R.E.N. Impens, K. Possemiers, E.F. Vansant, *J. Chem. Soc., Faraday Trans.* 92 (1996) 4285.
- [145] N.R.E.N. Impens, E.F. Vansant, *Interface Sci.* 5 (1997) 95.
- [146] L. Chmielarz, P. Kuśtrowski, R. Dziembaj, P. Cool, E.F. Vansant, *Appl. Catal. B: Environ.* 62 (2006) 369.
- [147] Y. Segura, L. Chmielarz, P. Kuśtrowski, P. Cool, R. Dziembaj, E.F. Vansant, *Appl. Catal. B: Environ.* 61 (2005) 69.
- [148] P. Van der Voort, J. Swerts, K.C. Vrancken, E.F. Vansant, P. Geladi, P. Grobet, *J. Chem. Soc., Faraday Trans.* 89 (1993) 63.
- [149] N.R.E.N. Impens, K. Schrijnemakers, E.F. Vansant, P. Grobet, J. Riga, O. Brouxon, *J. Mater. Chem.* 7 (1997) 1467.
- [150] I. Gillis-D'Hamers, K.C. Vrancken, E.F. Vansant, G. de Roy, *J. Chem. Soc., Faraday Trans.* 88 (1992) 2047.
- [151] I. Gillis-D'Hamers, J. Philippaerts, P. Van der Voort, E. Vansant, *J. Chem. Soc., Faraday Trans.* 86 (1990) 3747.
- [152] O. Collart, P. Van Der Voort, E.F. Vansant, E. Gustin, A. Bouwen, D. Schoemaker, R.R. Rao, B.M. Weckhuysen, R.A. Schoonheydt, *Phys. Chem. Chem. Phys.* 1 (1999) 4099.
- [153] P. Van der Voort, K. Possemiers, E.F. Vansant, *J. Chem. Soc., Faraday Trans.* 92 (1996) 843.
- [154] P. Van der Voort, I.V. Babitch, P.J. Grobet, A.A. Verberckmoes, E.F. Vansant, *J. Chem. Soc., Faraday Trans.* 92 (1996) 3635.
- [155] M. Baltes, P. Van Der Voort, B.M. Weckhuysen, R.R. Rao, G. Catana, R.A. Schoonheydt, E.F. Vansant, *Phys. Chem. Chem. Phys.* 2 (2000) 2673.
- [156] P. Van Der Voort, R. van Welzenis, M. de Ridder, H.H. Brongersma, M. Baltes, M. Mathieu, P.C. van de Ven, E.F. Vansant, *Langmuir* 18 (2002) 4420.
- [157] Y. Segura, L. Chmielarz, P. Kuśtrowski, P. Cool, R. Dziembaj, E.F. Vansant, *J. Phys. Chem. B* 110 (2006) 948.
- [158] J. Philippaerts, E.F. Vansant, G. Peeters, E. Vanderheyden, *Anal. Chim. Acta* 195 (1987) 237.
- [159] Y. Yan, J. Verbiest, P. de Hulsters, E.F. Vansant, *J. Chem. Soc., Faraday Trans.* 1 (85) (1989) 3095.
- [160] F. Goovaerts, E.F. Vansant, P. de Hulsters, J. Gelan, *J. Chem. Soc., Faraday Trans.* 1 (85) (1989) 3687.
- [161] M. Benjelloun, P. Cool, P. Van Der Voort, E.F. Vansant, *Phys. Chem. Chem. Phys.* 4 (2002) 2818.
- [162] Z. Hu, E.F. Vansant, *Carbon* 33 (1995) 1293, Carbon-aluminosilicate composite adsorbent.
- [163] P. Kuśtrowski, L. Chmielarz, R. Dziembaj, P. Cool, E.F. Vansant, *J. Phys. Chem. A* 109 (2005) 330.
- [164] P. Kuśtrowski, L. Chmielarz, R. Dziembaj, P. Cool, E.F. Vansant, *J. Phys. Chem. B* 109 (2005) 11552.
- [165] P. Van Der Voort, M. Baltes, E.F. Vansant, *Catal. Today* 68 (2001) 119.
- [166] K. Schrijnemakers, E.F. Vansant, *J. Porous Mater.* 8 (2001) 83.
- [167] S. Van Doorslaer, Y. Segura, P. Cool, *J. Phys. Chem. B* 108 (2004) 19404, TiO<sub>x</sub>–VO<sub>x</sub> mixed oxides on SB-15 support.
- [168] Y. Segura, P. Cool, P. Van Der Voort, F. Mees, V. Meynen, E.F. Vansant, *J. Phys. Chem. B* 109 (2004) 3794.
- [169] V. Meynen, Y. Segura, M. Mertens, P. Cool, E.F. Vansant, *Microporous Mesoporous Mater.* 85 (2005) 119.
- [170] Y. Segura, P. Cool, P. Kuśtrowski, L. Chmielarz, R. Dziembaj, E.F. Vansant, *J. Phys. Chem. B* 109 (2005) 12071.
- [171] P. Kuśtrowski, Y. Segura, L. Chmielarz, J. Surman, R. Dziembaj, P. Cool, E.F. Vansant, *Catal. Today* 114 (2006) 307.
- [172] G. Busca, *Catal. Today* 27 (1996) 323.